Accepted Manuscript

Toughening of high performance tetrafunctional epoxy with poly(allyl amine) grafted graphene oxide

Megha Sahu, Ashok M. Raichur

PII: S1359-8368(18)32986-X

DOI: https://doi.org/10.1016/j.compositesb.2018.12.030

Reference: JCOMB 6359

To appear in: *Composites Part B*

Received Date: 10 September 2018

Revised Date: 27 November 2018

Accepted Date: 11 December 2018

Please cite this article as: Sahu M, Raichur AM, Toughening of high performance tetrafunctional epoxy with poly(allyl amine) grafted graphene oxide, *Composites Part B* (2019), doi: https://doi.org/10.1016/j.compositesb.2018.12.030.

Toughening of high performance tetrafunctional epoxy with poly(allyl amine) grafted graphene oxide

Megha Sahu[†], Ashok M. Raichur[§†*]

[†]Department of Materials Engineering, Indian Institute of Science, Bangalore, 560012, India

[§]Nanotechnology and Water Sustainability Research Unit, University of South Africa, The Science Campus, Florida Park, 1710 Roodepoort, Johannesburg, South Africa

Abstract

The mechanical and thermal properties of epoxy composites were improved by using poly(allyl amine) (PAA) grafted graphene oxide (GO) as a toughening agent. The GO was first converted to GO-COOH where all the hydroxyl groups on the basal plane were converted to COOH containing groups. GO-COOH was reacted with PAA to yield GO-g-PAA. The effect of PAA grafted GO nanosheets as fillers on mechanical and thermal properties of aerospace grade epoxy was studied. Epoxy nanocomposites containing graphene oxide (GO) and GO-g-PAA nanosheets were fabricated by incorporating 0.35 to 1.4 wt% of filler. GO-g-PAA modified epoxy nanocomposites showed excellent improvement in flexural, compression and fracture properties compared to neat epoxy and GO modified epoxy. Fracture toughness increased from 0.94 MPa $m^{-1/2}$ for neat epoxy to 1.75 MPa $m^{-1/2}$ (87%) for epoxy nanocomposites modified with 0.7 wt% of GO-g-PAA nanosheets. The temperature for 5% weight loss showed drastic improvement of 24 °C for epoxy nanocomposites modified with 0.7 wt% of GO-g-PAA nanosheets. The examination

[*]Corresponding author. Email: amr@iisc.ac.in Fax: +91-80-23600472; Tel: +91-80-22933238

of fractured surfaces of modified epoxy nanocomposites showed better interaction of GO-g-PAA nanosheets with epoxy compared to GO nanosheets.

Keywords: Polymer-matrix composites, Fracture toughness, Thermosetting resin, Nano-structures.

1. Introduction

Epoxy composites have created a niche for itself in aerospace and automotive industries. Epoxy, in the form of carbon fiber reinforced polymers (CFRP), is used in structural parts of aircrafts. Boeing 787 and Airbus 350 have advanced polymer composites which make ~50% of the total material used in the aircraft. The fuselage i.e. main body of these aircrafts is made of epoxy-based composites. Bifunctional epoxies i.e. epoxy resin having two terminal epoxy functionalities, have lower thermal and mechanical properties hence only tetrafunctional epoxy polymers are used for fabrication of structural parts of an aircraft. Tetrafunctional epoxy polymers have four functional groups which result in higher degree of crosslinking. The glass transition temperature (T_g) of tetrafunctional epoxy polymers varies from 200-280 °C which is much higher than the T_g of conventional bifunctional epoxy polymers. However, due to high degree of crosslinking of tetrafunctional epoxy polymers, the structure becomes extremely rigid and prone to fracture in the presence of manufacturing defects. Hence, improving the fracture properties of multifunctional epoxy polymers is significantly important.

Graphene and its modified forms have been explored extensively for improving mechanical[1-4] and thermal[5, 6] properties of epoxy polymers due to their unique

properties such as high strength[7], thermal properties (~5000 W m^{-1} k^{-1})[8], electric properties (mobility of charge carriers-200,000 cm^2 g^{-1})[9] and superior specific surface area (2630 m^2 g^{-1})[10]. Excellent improvement in fracture properties[11-14] has been reported using extremely low weight percent of graphene and GO. Due to the presence of oxygen functional groups on GO, it has good compatibility with epoxy polymer as these groups are capable of forming chemical bonds with epoxy matrix.

Despite being chemically compatible with epoxy, dispersion of the GO nanosheets in epoxy is a challenge. GO does not disperse well in weakly polar solvents which are compatible with epoxy. Hence, functionalization of GO helps in overcoming the issue of dispersion of GO in suitable solvent. Many researchers studied the effect of epoxy[6, 15], silica[16, 17] and amine[15, 18-22], functionalized GO and graphene for improving mechanical properties of epoxy. Various amine functionalized[23-30] molecules have been grafted onto GO for improved mechanical and thermal properties of epoxy nanocomposites. In all covalent modifications, molecules are attached only to the edges of GO sheets. In the functionalization reaction, amide linkage is formed because of reaction between amine groups of the functionalizing molecule and carboxylic acid groups of GO. This is because of the presence of carboxylic acid groups only at the edges of GO (Lerf-Klinowski model[31]) which results in restricted functionalization with amine groups containing molecules on edges of GO nanosheets[23-30]. Hence, the adhesion of sheets to epoxy matrix is limited which results in weaker interlocking between epoxy and filler. The presence of amine groups on the surface as well as on the edges is expected to result in a stronger interface and better reinforcement of epoxy nanocomposites.

In the present study, GO nanoplatelets have been modified with poly(allyl amine) (PAA) which has a higher density of amine groups per molecule compared to conventionally used bifunctional amine molecules. This helps in formation of larger number of chemical bonds between epoxy and amine functionalized GO. GO nanoplatelets have been modified such that it results in presence of carboxylic acid groups (COOH) at their basal plane. Carboxyl functionalized GO (GO-COOH) is formed after converting epoxy groups of GO basal plane to carboxyl groups, using chloroacetic acid and sodium hydroxide[32]. This ensures the presence of amine groups at the basal plane and not only at the edges of GO. The presence of COOH at the basal plane and grafting of PAA polymer chain with high number of amine groups improved the dispersion and interaction between functionalized GO and epoxy matrix. The GO-g-PAA modified epoxy showed excellent improvement in mechanical and thermal properties of epoxy nanocomposites compared to both GO modified and neat epoxy. The filler-matrix interaction was studied by fractographic analysis.

2. Materials and Methods

2.1 Materials

Natural flake graphite (45 µm) and Poly(allyl amine hydrochloride) (PAA, Mw 56000) were purchased from Sigma-Aldrich Co. (USA). *N*,*N*′-dicyclohexylcarbdiimide (DCC), N-hydroxysuccinimide (NHS), Sulfuric acid (H_2SO_4, 98%) and Hydrochloric acid (HCl, 35% in water) were purchased from Sisco Research Laboratories (SRL) Pvt. Ltd. (India). Sodium hydroxide (NaOH), Chloroacetic acid ($ClCH_2COOH$), Potassium per magnate ($KMnO_4$), Hydrogen peroxide (H_2O_2, 30%), sodium nitrate ($NaNO_3$) and Triethylamine (TEA) were purchased from S. D. Fine-Chem Ltd. (India). Epoxy, *N*,*N*,*N*′,*N*′-tetraglycidyl-

4,4'-methylenebisbenzenamine (TGDDM, Araldite MY 721) and curing agent *4,4'*-diaminodiphenylsulfone (DDS, Aradur 9664) were purchased from Huntsman Advanced Materials (Huntsman Corporation, USA). Double autoclaved Milli-Q water (Millipore, Billerica, MA, USA) produced in the lab was used in all the experiments.

2.2 Synthesis of GO-COOH

Graphite oxide was synthesized by oxidizing natural graphite flakes by following modified Hummers method[33]. Briefly, 1 g of graphite oxide was added to a 250 ml of DI water. The mixture was sonicated for 2 h to exfoliate the GO sheets from graphite oxide platelets. Then, 23 g of NaOH and 20 g of Chloroacetic acid was dissolved in 40 ml of DI water separately. The GO suspension was mixed with NaOH and Chloroacetic acid[32]. The mixture was stirred for 3 h at room temperature. The GO agglomerated in the presence on NaOH. Then, precipitate was collected by centrifuging the mixture. The final product was washed with DI water and ethanol several times. GO-COOH obtained as a result of the reaction was dried at 50 ° for 12 h.

2.3 Synthesis of GO-g-PAA

GO-COOH (0.8 g) was dispersed in DI water (120 ml) with the aid of bath sonication for 0.5 h. Then, 0.4 g of PAA was dissolved in 25 ml of DI water in a separate beaker. GO-COOH suspension and PAA solution were transferred to 500 ml round bottom flask and the mixture was stirred for 0.5 h. TEA (2.5 ml) was added to the mixture. To the mixture, 0.4 g of EDC and 0.2 g of NHS were added and refluxed for 24 h at 70 °C. The reaction product was collected by centrifuging the mixture. GO-g-PAA obtained as reaction product was washed several times with DI water and ethanol. The product was dried at 50 °C for 24 h.

2.4 Fabrication of Epoxy/GO and Epoxy/GO-g-PAA nanocomposites

GO-g-PAA nanosheets were dispersed in ethanol (10 mg/ml) using bath sonication for 2 h. In a separate beaker, epoxy was heated up to 80 °C with continuous stirring to reduce its viscosity. GO-g-PAA nanosheets suspension was added to epoxy and the mixture was stirred at high speed to ensure homogeneous distribution of the nanosheets. To get rid of the residual solvent, the epoxy mixture was kept in vacuum oven for 12 h at 90 °C. Then, epoxy mixture was heated at 120 °C with stirring and stoichiometric amount of curing agent was added. The mixture was subjected to high speed stirring for uniform distribution of the curing agent. To get rid of the air bubbles introduced during high speed stirring, epoxy mixture was degassed in vacuum oven at 90 °C for 2 h. Finally, the epoxy mixture was poured in preheated mold and cured at 150 °C for 2h, 180 °C for 2h and 200 °C for 2 h. Epoxy nanocomposites containing 0.35, 0.7, 1.05 and 1.4 wt% of GO-g-PAA and GO nanosheets were fabricated. Neat epoxy samples were fabricated for comparison.

2.5 Characterization methods

The morphology of GO, GO-g-PAA and fractured epoxy samples from the mechanical tests were analyzed using Scanning Electron Microscope (SEM, FEI Sirion XL30 FEG, FEI, Oregon, USA). Samples were coated with 10 nm thick layer of gold coating to impart conductivity. The difference in morphology of GO and GO-g-PAA was studied by Transmission Electron Microscopy (JEOL 2000 FX-II TEM, JEOL, Akishima, Tokyo, Japan). Nanosheets were dispersed in water with the help of sonication and a drop from the obtained suspension was casted on a carbon coated Cu grid. Samples were dried and desiccated prior to analysis. FTIR spectra of GO, PAA and GO-g-PAA were recorded on

Thermo-Nicolet 6700 FTIR spectrometer (Thermo Fisher Scientific, Waltham, Massachusetts, USA) in 400-4000 cm^{-1} region. Powdered samples were incorporated in KBr discs for the analysis. Thermal stabilities of GO, GO-g-PAA and epoxy/GO-g-PAA nanocomposites were studied by performing thermo-gravimetric analysis (TGA) on a NETZSCH STA 409 (NETZSCH-Gerätebau GmbH, Selb, Germany). 5-10 mg of samples were heated from room temperature to 800 °C at the rate of 10 °C min^{-1} under Argon atmosphere. X-ray powder diffraction was conducted to study the difference in the crystal structure of GO and GO-g-PAA. The measurement was conducted at a scan speed of 2° min^{-1} between 5-80° using X-Pert PRO (PANalytical, Almedo, The Netherlands) equipped with Cu K α tube. Raman spectra of GO and GO-g-PAA were obtained on a LabRAM HR (Horiba Scientific Ltd, Kyoto, Japan) equipped with 514 nm laser. Dynamic mechanical analysis of epoxy nanocomposites was done on a Gabo eplexor 500N (NETZCSH Gabo Instruments GmbH, Ahlden, Germany). Samples with dimensions 5 × 2 × 45 mm^3 were used. The samples were subjected to 3-point bend tests with the frequency of 1 Hz and temperature varied from 30 °C to 330 °C at the rate of 3 °C min^{-1}. Compression testing was performed according to ASTM D695 with a Zwick/Rowell Z100 machine (Zwick Roell, Ulm, Germany). Samples with cylindrical geometries having diameter 6.9 mm and length 10.4 mm were used for the testing. Cross-sectional area of each sample was polished with P4000 grade emery paper to remove the mold imprints. Five replicas of each sample were tested, and the average value was reported. Flexural properties of the nanocomposites were tested by performing 3-point bend tests on a Zwick /Rowell Z100 (Zwick Roell, Ulm, Germany) by following ASTM D790. Samples with dimensions 48 × 3 × 12 mm^3 were used. Five replicas of each composition were tested. Fracture toughness of the

nanocomposites was obtained by performing single edge notch bend test according to ASTM D5045. Rectangular samples with dimension 6 ×12 × 48 mm^3 were tested on Zwick/Rowell Z100 (Zwick Roell, Ulm, Germany). A notch watch induced by machining and natural crack was grown in each sample by tapping a razor blade pre-cooled in liquid N_2. Fracture toughness (K_{IC}) was calculated using the following relationship.

$$K_{IC} = \frac{P_{max}}{BW^{1/2}} f(a/W) \quad (1)$$

Where P_{max} is the maximum load of the load-displacement curve, W is the width of the sample, B is the thickness of the 3-point bend sample, and a is the length of the pre-crack. f(a/W) is a geometry dependent function given by following equation.

$$f\left(\frac{a}{W}\right) = 6x^{1/2} \frac{[1.99-x(1-x)(2.15-3.93x+2.7x^2)]}{(1+2x)(1-x)^{3/2}} \quad (2)$$

Six replicas of each composition were tested and the average value was reported.

3. Results and Discussion

3.1 Synthesis and characterization of GO and GO-g-PAA

GO synthesized via Hummers method has carboxyl groups acid groups at the edges. To induce the presence of carboxyl groups on the basal plane of GO, it was modified with the help of NaOH and chloroacetic acid[32]. NaOH provides the necessary basic condition for the reaction. The reaction between GO and chloroacetic acid converts hydroxyl groups of

the basal plane of GO to COOH groups. COOH groups present at the basal plane of GO-COOH helps in grafting of PAA chains through formation amide bonds. PAA was chosen to modify surface of GO as it contains high density of amine groups per polymer chain. This helps in formation of greater number of chemical bonds between epoxy and amine functionalities of GO. This leads to better interlocking and stronger interface between GO and epoxy matrix. The bulky nature of PAA chains also helps in prevention of agglomeration of sheets due to van der Waals forces among GO nanosheets. Figure 1 (a) shows the schematic diagram of synthesis of GO-COOH and GO-g-PAA. Figure 1 also shows incorporation of GO-g-PAA nanosheets in epoxy matrix.

The morphology of GO and GO-g-PAA nanosheets was characterized by SEM. Figure 2 (a) and (b) show SEM micrographs of GO and GO-g-PAA respectively. High level of wrinkles and folding of sheets observed in SEM micrograph of GO-g-PAA indicates higher level of defect formation due to presence of PAA molecules. The nanosheets appear well exfoliated in case of both GO and GO-g-PAA. Figure 2 (c) and (d) shows TEM micrographs of GO and GO-g-PAA. GO nanosheets have highly transparent structure due to their few atom thick structure. However, GO-g-PAA nanosheets appear less transparent which could be attributed to the presence of bulky PAA polymeric chain on the surface of GO-g-PAA nanosheets.

FTIR spectroscopy was conducted to confirm the changes in chemical structure of GO after functionalization. Figure 3 (a) shows the FTIR spectra of GO, PAA and GO-g-PAA nanosheets. The absorption bands appear at 1056 cm^{-1} (C-O-C stretch), 1622 cm^{-1} (C=C stretch), 1727 cm^{-1} (C=O stretch) and 3347 cm^{-1} (O-H stretch) for GO which confirm the oxidation of graphite carried out by modified Hummer's method. FTIR spectrum of PAA

shows characteristic peaks of N-H stretch of amine groups at 3427 cm^{-1}. The peaks corresponding to N-H symmetrical and asymmetrical bend are observed at 1615 $cm^{-1}$and 1510 cm^{-1} respectively. The peak for C-H stretching of the carbon backbone of PAA polymeric chains is observed at 2935 cm^{-1}. FTIR spectrum of GO-g-PAA shows characteristic peaks of both GO and PAA. The characteristic peak of N-H stretching is observed at 3428 cm^{-1}.

The difference in the interplanar spacing of graphite, GO and GO-g-PAA was studied by XRD analysis. Figure 3 (b) shows the XRD spectra of graphite, GO and GO-g-PAA. For natural graphite, the peak at 26.2° observed for (002) corresponds to interplanar spacing of about 0.34 nm. However, the interplanar spacing shows a significant increase due to expansion of (002) planes by introduction of several oxygen containing functional groups during formation of GO. This is confirmed by appearance of (002) peak at 10.6° for GO which corresponds to interplanar spacing of about 0.83 nm. GO shows significant reduction in the intensity of (002) peak accompanied with broadening of peak, compared to graphite. This could be attributed to the reduction of the crystallite size due to exfoliation of sheets. GO-g-PAA was expected to show further increase in interplanar spacing due to anchored chains of PAA. This was confirmed by XRD spectrum of GO-g-PAA as (002) peak appeared at 10.2° that corresponds to an interplanar spacing of 0.87 nm. The intensity of the (002) peak also showed a drastic reduction and peak showed further broadening which could be attributed to the reduction in the crystallite size due to exfoliation owing to the presence of PAA chains on the surface of GO. Larger interplanar spacing, decrease in the intensity and broadening of peaks suggest successful functionalization of the PAA chains onto GO nanosheets.

Raman spectra of graphite, GO and GO-g-PAA are shown in Figure 3 (c). Graphite shows a very weak band at 1352 cm^{-1} and a strong band at 1580 cm^{-1}. These correspond to D and G band respectively. D band arises from basal plane defects and edge of graphitic structure whereas G band arises from radial C-C stretching mode associated with sp^2 hybridized carbon atoms of honeycomb lattice. Since the defects in the natural graphite are less compares to GO, the intensity of the D band of graphite is very low compared to GO and GO-g-PAA. GO shows significant increase in the intensity of D band indicating introduction of defects in the lattice due to distortion of the bonds. It is well documented that ratio of intensity of D and G band (I_D/I_G) depicts the extent of defects in the GO and modified GO. Compared to GO, the I_D/I_G value of GO-g-PAA shows slight increase from 0.98 to 1.03 which could be due to enhanced defect owing to the formation of new bonds between GO and PAA molecules.

Thermogravimetric analysis was conducted to further confirm the functionalization of GO with PAA. Figure 3 (d) shows the TGA curves for graphite, GO and GO-g-PAA. Graphite consists of tightly packed layers of sp^2 hybridized carbon. Hence the thermal stability of graphite is high. Graphite gets oxidized at temperatures as high as 700 °C. As expected, graphite showed high thermal stability as no weight loss took place until 700 °C. However, GO showed 20% weight loss at 129 °C and underwent rapid weight loss at 145 °C due to loss of oxygen functionalities such as OH and COOH. GO-g-PAA showed a 50% weight loss at 410 °C which is 114 °C higher than that for GO. This could be attributed to functionalization of PAA chains onto GO by replacing oxygen functionalities. PAA molecules being a polymer have higher thermal stability as compared to oxygen

functionalities. Hence, Higher thermal stability of GO-g-PAA compared to GO indicates successful functionalization of GO with PAA.

3.2 Thermal stabilities of Epoxy/GO and Epoxy/GO-g-PAA nanocomposites

Figure 4 (a) and (b) shows the TGA results of Epoxy/GO, Epoxy/GO-g-PAA nanocomposites and neat epoxy. The key data is listed in Table 1. All the fabricated samples show similar thermal decomposition behavior as the major weight loss takes place in a single step in the temperature range 300-450 °C. The results show that thermal stability of epoxy nanocomposite is significantly affected due to the presence of both GO and GO-g-PAA nanosheets. The temperature for 5% weight loss ($T_{-5\%}$) shows significant increase for loading up to 1.05 wt% in case of GO and GO-g-PAA modified epoxy nanocomposites. The incorporation of GO and GO-g-PAA beyond 1.05 wt% leads to $T_{-5\%}$ values similar to that of neat epoxy. For example, maximum improvement in $T_{-5\%}$ was obtained by incorporation of 0.7 wt% of GO and GO-g-PAA. Epoxy modified with 0.7 wt% of GO showed 39 °C increase in $T_{-5\%}$ whereas epoxy modified with 0.7 wt% GO-g-PAA showed 23 °C increase in $T_{-5\%}$ compared to neat epoxy. Similarly, incorporation of 1.05 wt% of GO showed 28 °C increase in $T_{-5\%}$ and incorporation of GO-g-PAA showed 22 °C improvement in $T_{-5\%}$ compared to neat epoxy. GO modified epoxy nanocomposites show maximum improvement in $T_{-5\%}$ at 0.7 wt% and exhibit a 10 °C decrease when loading is further increased to 1.05 wt%. This could be attributed to reduction in the extent of distribution of GO sheets in epoxy matrix. However, GO-g-PAA modified epoxy nanocomposites show similar improvement in $T_{-5\%}$ for 0.7 and 1.05 wt% (Table 1). This could be attributed to uniform distribution and improved interaction of GO-g-PAA nanosheets with epoxy even at

loading as high as 1.05 wt%. The results show that epoxy nanocomposites exhibit significant improvement in thermal properties on incorporation of GO and GO-g-PAA nanosheets. This improvement in thermal stabilities could be attributed to the barrier effect of GO and GO-g-PAA owing to their robust structure and large aspect ratio. The GO and GO-g-PAA nanosheets restrict the volatilization of polymer network which delays the thermal degradation process.

3.3 Dynamic mechanical analysis

High T_g and undisputed excellent mechanical performance are few of the major reasons for tetrafunctional epoxies to be one of the most used polymer matrices for reinforced composites in aerospace industry. Hence, it is of utmost importance that improvement in mechanical properties is not achieved at the cost of thermal properties like in case of rubber toughened epoxy polymers. To ensure that the thermal properties of the GO-g-PAA modified epoxy nanocomposites are as good as or better than unmodified epoxy, dynamic mechanical analysis was conducted. Figure 5 (a-d) shows the plots of variation of storage modulus and tan δ as a function of temperature for epoxy and modified epoxy nanocomposites and the key data is listed in Table 1. The storage modulus values at temperatures below T_g of the nanocomposites indicates the extent of reinforcement by the filler. Clearly, incorporation of GO does not affect the storage modulus of the nanocomposites to a noticeable extent as seen in Figure 5 (a). The storage modulus of GO modified epoxy nanocomposites for all the compositions show values similar to neat epoxy for temperatures ranging from 150 °C to 200 °C. The largest improvement of 25 % in storage modulus was observed at 250 °C for epoxy nanocomposite with 0.35 wt% of GO

compared to neat epoxy. Epoxy nanocomposites modified with GO-g-PAA nanosheets show significant improvement in storage modulus for temperature range both below and above T_g Figure 5(c)). The storage modulus of epoxy nanocomposite modified with 0.7 wt% GO-g-PAA showed 34% improvement at 150 °C compared to neat epoxy. Similarly, Epoxy/GO-g-PAA (0.7 wt%) showed 36% and 56% improvement in storage modulus at 200 °C and 250 °C respectively compared to neat epoxy. The extent of improvement decreases when GO-g-PAA loading is increased beyond 0.7 wt%. However, the improvement in the storage modulus observed for GO-g-PAA modified epoxy is significantly higher than that for GO modified epoxy and neat epoxy. The increase in the storage modulus is attributed to restriction of mobility of the polymeric chains due to formation of larger number of chemical bonds between GO-g-PAA and epoxy owing to the presence of PAA chains as connecting links. Whereas, in case of GO the covalent bond formation is restricted to only edges of GO sheets. This is due to presence of COOH groups only at the edges of the sheets. Hence GO sheets are much less efficient in providing a barrier to movement of epoxy molecular chain. For the analysis of glass transition temperatures of modified and unmodified epoxy, T_g was taken as the maximum peak value of tan δ versus temperature curves (Figure 5 (b) and (d)). GO modified epoxy exhibited T_g values similar to that of neat epoxy up to loading of 0.7 wt%. Figure 5 (b). T_g shows a minor increase of ~3 °C for epoxy modified with GO-g-PAA nanosheets. None of the fabricated compositions of GO-g-PAA modified epoxy polymers showed reduction in T_g as seen in Figure 5 (d). This could be attributed to restricted conformational changes of epoxy chains owing to the presence of GO-g-PAA nanosheets facilitated by extensive covalent

bonding via PAA linker chains. This restricted motion of epoxy chains delays the glass transition compared to neat epoxy.

3.4 Mechanical properties of Epoxy/GO and Epoxy/GO-g-PAA nanocomposites

3.4.1 Compressive and flexural properties

Figure 6 (a) and (b) show the representative stress versus strain curves of compression tests for Epoxy/GO and Epoxy/GO-g-PAA nanocomposites respectively. The strain at break shows an improvement of ~20 % for epoxy modified with low loading of GO nanosheets (0.35 and 0.7 wt%) compared to neat epoxy. Epoxy nanocomposites modified with higher loading (1.05 and 1.4 wt%) of GO show strain at load comparable to neat epoxy. The strain at break shows 75% increase for epoxy modified with GO-g-PAA nanosheets compared to neat epoxy. This could be attributed to well dispersed GO-g-PAA sheets which are covalently anchored via PAA linker chains to epoxy by its edges as well as basal plane. The dangling chains of PAA make the epoxy-GO interlocking less rigid and allow easy flow of matrix under compressive load. The compressive strength versus filler content plot in Figure 6 (c) shows that GO modified epoxy nanocomposites exhibit maximum improvement of 19% in compressive strength at loading level of 0.7 wt%. Incorporation of GO sheets beyond 0.7 wt% leads to compressive strength values similar to neat epoxy. This could be due to reduction in the dispersion level of GO sheets in the absence of any bulky groups to prevent agglomeration of sheets inside polymer matrix at higher loading levels. Contrary to this, GO-g-PAA modified epoxy nanocomposites showed significant improvement in compressive properties for all the compositions

compared to neat epoxy. The maximum improvement in compressive strength was observed for epoxy nanocomposites modified with 1.05 wt% of GO-g-PAA nanosheets. On incorporation of 1.4 wt% of GO-g-PAA nanosheets, reduction in the extent of improvement is observed. However, even at higher level of loading of GO-g-PAA, compressive properties show significant improvement compared to neat epoxy and GO modified epoxy. The striking difference in the compressive behavior of GO and GO-g-PAA modified epoxy could be attributed to the degree of dispersion of nanosheets and extent of interaction of nanosheet with epoxy matrix. GO-g-PAA owing to the presence of PAA molecules with compatibilizing amine groups at basal plane and edges allows better bonding with the matrix. This results in better load transfer during compressive loading of epoxy samples. The bulky nature of PAA polymeric chains also prevents agglomeration upon incorporation of GO-g-PAA nanosheets at high wt% (1.05, 1.4 wt%). GO nanosheets in the absence of bulky groups on its basal plane leads to agglomeration in epoxy matrix. Hence, GO modified epoxy nanocomposites show saturation at loading of 1.0 wt% or more.

Flexural properties also showed similar behavior, as GO modified epoxy nanocomposites showed improvement up to 0.7 wt% loading of GO nanosheets. GO-g-PAA modified epoxy nanocomposites showed improvement for all the compositions as shown in Figure 6 (d). GO modified epoxy nanocomposites showed maximum improvement of 41% in flexural strength for loading of 0.7 wt%. However, epoxy nanocomposites showed drastic decrease in flexural strength value when loading of GO was increased beyond 0.7 wt%. Epoxy nanocomposites modified with 0.7 wt% of GO-g-PAA nanosheets showed maximum improvement of 43% in the flexural strength which was maintained up to loading levels of 1.05 wt%. However, the extent of improvement in flexural strength

showed decrease from 40% for 1.05 wt% to 10 % for 1.4 wt% loading of GO-g-PAA nanosheets. The significant improvement in flexural properties of GO-g-PAA nanosheets modified epoxy nanocomposites could be attributed to (i) intrinsic high strength and flexibility of GO-g-PAA sheets, (ii) improved filler-matrix interaction due to presence of covalently bonded PAA chains leading to stronger interfaces and (iii) uniform distribution even at loading as high as 1 wt%.

3.4.2 Fracture properties

Fracture properties of Epoxy/GO and Epoxy/GO-g-PAA nanocomposites were studied by performing single edge notch bend (SENB) test. Figure 7 (a) shows typical load versus displacement curves of fracture toughness tests for neat epoxy, Epoxy/GO nanocomposites and Epoxy/GO-g-PAA nanocomposites for selective compositions. Clearly, GO-g-PAA modified epoxy nanocomposites withstand higher loads compared to GO modified epoxy nanocomposites and neat epoxy. (b) compares the fracture toughness values of neat epoxy, GO and GO-g-PAA modified epoxy nanocomposites. Neat epoxy exhibits fracture toughness of 0.94 MPa $m^{-1/2}$. Incorporation of 0.35 wt% of GO results in 43% increase in K_{IC} compared to neat epoxy. The improvement on further increasing loading of GO to 0.7 wt% remains similar to that of 0.25 wt% loading. Other research groups have reported similar results and have shown that unfunctionalized GO shows improvement only up to loading ????[34-36]. However, with addition of GO beyond 0.7 wt% sharp decrease in extent of improvement is observed. This is well reported that GO modified epoxy nanocomposites show improvement with loading of GO up to 0.5 wt% and show saturation or degradation of fracture properties on addition of GO sheets beyond this level[1, 12, 37-

39]. Addition of GO-g-PAA nanosheets at 0.35 wt% showed significant improvement of 80% compared to neat epoxy. The fracture toughness further showed 87% improvement with incorporation of 0.7 wt% of GO-g-PAA nanosheets. This level improvement was maintained on addition of GO-g-PAA nanosheets at loading as high as 1.4 wt%. This improvement could be attributed to (i) robust nature of GO-g-PAA nanosheets, (ii) better interlocking owing to the presence of compatibilizing PAA chains GO-g-PAA nanosheets, (iii) improved adhesion of GO sheets to epoxy matrix owing to the presence of PAA chains at basal plane and not only at the edges and (iv) improved dispersion of GO-g-PAA due to presence of bulky polymeric chains on the basal plane which inhibits agglomeration at higher loading level in epoxy matrix. The toughening mechanism of graphene is similar to silica like rigid materials. Graphene provides stronger interfaces and resists crack propagation. There are mainly two mechanisms for toughening of epoxy by graphene as suggested by S. Chandrasekaran *et. al.*[40]. One of the mechanisms includes crack pinning and the other involves crack deflection. Crack pinning results in bifurcation of crack front and crack grows on either side of the graphene sheet. The two crack fronts meet ahead of the graphene sheet resulting in uneven fractured surface.

The poor toughening effect and saturation of improvement at relatively low loading of GO could be attributed to absence of compatibilizing groups on the surface of GO which leads to poor adhesion of sheets to epoxy matrix. Poor adhesion leads to relatively ineffective load transfer during mechanical loading which is reflected in comparatively low fracture toughness values of GO modified epoxy relative to GO-g-PAA modified epoxy at similar loading levels.

3.4.3 Study of Fractured Surfaces

Fractographic analysis was performed by scanning electron microscopy to find out the extent of interaction of GO and GO-g-PAA nanosheets with epoxy matrix. Figure 8 shows SEM micrographs of cross-sectional areas of fractured samples of epoxy nanocomposites. It can be seen in Figure 8 (a) and (b) that neat epoxy samples have a highly smooth and uniform surfaces characteristic of a brittle failure. Figure 8 (c) and (d) show the surface morphology of fractured samples of Epoxy/GO (0.35 wt%) and Epoxy/GO-g-PAA (0.35 wt%) respectively. It can be observed that both the samples show highly rough and non-uniform surfaces which results in high load at fracture for modified samples. However, a closer look at the Epoxy/GO (0.35 wt%) shows stacked sheets of GO embedded in epoxy matrix. This could be due to poor dispersion of GO in ethanol which leads to poor exfoliation and hence dispersion of multilayered GO sheets in epoxy. However the fracture toughness value for Epoxy/GO (0.35 wt%) is still better than neat epoxy. Although GO is poorly exfoliated and dispersed, the GO sheets are still able to make the interface stronger to withstand higher level of mechanical loading [41]. As seen in Figure 8(d), Epoxy/GO-g-PAA (0.35 wt%) shows good adhesion of GO-g-PAA nanosheets to epoxy matrix as there are no lose sheets visible. For higher loading of GO and GO-g-PAA nanosheets in epoxy, Figure 8 (e-j), epoxy samples with GO-g-PAA nanosheets show more uneven morphology compared to neat and GO modified epoxy nanocomposites. This could be attributed to better interlocking between epoxy and GO-g-PAA nanosheets owing to the presence of PAA chains which helps in formation of larger number of covalent bonds between GO-g-PAA and epoxy. Another reason could be enhanced defect structure in GO sheets due to the

presence of bulky PAA chains all over its surface which give rise to enhanced wrinkly-like structures in the fractured surfaces. When the crack propagates, wrinkled surface of sheets adhering strongly to epoxy matrix, interrupts the crack growth which results in more tortuous path for crack propagation. Thus, higher values K_{IC} of GO-g-PAA modified epoxy compared to GO modified epoxy at higher loading levels could be explained by stronger chemical bonding of GO-g-PAA nanosheets with epoxy matrix and better exfoliation of GO-g-PAA in solvent assisted mixing leading to higher effective volume of GO-g-PAA nanosheets in epoxy matrix.

4. Conclusions

In this work, a new strategy for synthesizing amine functionalized GO was demonstrated which improves the extent of interaction of GO and its adhesion to epoxy matrix. GO was converted to GO-COOH and further functionalized with PAA to yield functionalization on the basal planes and edges of GO. Using basal plane functionalized GO as toughening agent lead to significant improvement in compression, flexural and fracture properties of epoxy nanocomposites. The addition of 1.05 wt% of GO-g-PAA nanosheets resulted in 50%, 40% and 76% improvement in compressive strength, flexural strength and fracture toughness respectively, compared to neat epoxy. The thermal properties also exhibited noticeable improvement as the $T_{-5\%}$ value showed increase of 24 °C on incorporation of 0.7 wt% of GO-g-PAA nanosheets. The storage modulus at 250 °C, which is near T_g of the material, showed excellent improvement of 56% with 0.7 wt% of GO-g-PAA nanosheets. The SEM analysis of fractured surfaces revealed good exfoliation, better adhesion of

nanosheets with the matrix and absence of loose sheets of GO-g-PAA in epoxy matrix which could be attributed to functionalization of GO with PAA using a different strategy.

Acknowledgements

The authors are grateful for the financial support from The Boeing Company. The authors wish to acknowledge CSIR for providing Megha Sahu with Senior Research Fellowship (SRF). The authors also acknowledge the support of technical staff of Department of Materials Engineering, the Advanced Facility for Microscopy and Microanalysis and Centre for Nano Science and Engineering at Indian Institute of Science for providing access to characterization facilities.

Supporting Information

Schematic illustration of Mechanism of synthesis of conventionally adopted edge functionalized GO and basal plane + edge functionalized GO (GO-g-PAA). SEM images of (a) GO and (b) GO-g-PAA. Digital image of GO and GO-g-PAA suspensions in ethanol (c) immediately after sonication and (d, f) 24 h after sonication.

Notes

The authors declare no competing financial interest.

References

[1] Rafiee MA, Rafiee J, Srivastava I, Wang Z, Song H, Yu Z-Z, et al. Fracture and Fatigue in Graphene Nanocomposites. Small. 2010;6(2):179-83.

[2] Zaman I, Phan TT, Kuan H-C, Meng Q, Bao La LT, Luong L, et al. Epoxy/graphene platelets nanocomposites with two levels of interface strength. Polymer. 2011;52(7):1603-11.
[3] Bortz DR, Heras EG, Martin-Gullon I. Impressive Fatigue Life and Fracture Toughness Improvements in Graphene Oxide/Epoxy Composites. Macromolecules. 2012;45(1):238-45.
[4] Chatterjee S, Nafezarefi F, Tai NH, Schlagenhauf L, Nüesch FA, Chu BTT. Size and synergy effects of nanofiller hybrids including graphene nanoplatelets and carbon nanotubes in mechanical properties of epoxy composites. Carbon. 2012;50(15):5380-6.
[5] Galpaya D, Wang M, George G, Motta N, Waclawik E, Yan C. Preparation of graphene oxide/epoxy nanocomposites with significantly improved mechanical properties. Journal of Applied Physics. 2014;116(5):53518.
[6] Wan Y-J, Tang L-C, Gong L-X, Yan D, Li Y-B, Wu L-B, et al. Grafting of epoxy chains onto graphene oxide for epoxy composites with improved mechanical and thermal properties. Carbon. 2014;69:467-80.
[7] Lee C, Wei X, Kysar JW, Hone J. Measurement of the Elastic Properties and Intrinsic Strength of Monolayer Graphene. Science. 2008;321(5887):385-8.
[8] Balandin AA, Ghosh S, Bao W, Calizo I, Teweldebrhan D, Miao F, et al. Superior Thermal Conductivity of Single-Layer Graphene. Nano Letters. 2008;8(3):902-7.
[9] Bolotin KI, Sikes KJ, Jiang Z, Klima M, Fudenberg G, Hone J, et al. Ultrahigh electron mobility in suspended graphene. Solid State Communications. 2008;146(9-10):351-5.
[10] Stoller MD, Park S, Zhu Y, An J, Ruoff RS. Graphene-based ultracapacitors. Nano letters. 2008;8(10):3498-502.
[11] Li Z, Wang R, Young RJ, Deng L, Yang F, Hao L, et al. Control of the functionality of graphene oxide for its application in epoxy nanocomposites. Polymer. 2013;54(23):6437-46.
[12] T.K BS, Nair AB, Abraham BT, Beegum PMS, Thachil ET. Microwave exfoliated reduced graphene oxide epoxy nanocomposites for high performance applications. Polymer. 2014;55(16):3614-27.
[13] Ma J, Meng Q, Michelmore A, Kawashima N, Izzuddin Z, Bengtsson C, et al. Covalently bonded interfaces for polymer/graphene composites. Journal of Materials Chemistry A. 2013;1(13):4255-64.

[14] Jiang T, Kuila T, Kim NH, Lee JH. Effects of surface-modified silica nanoparticles attached graphene oxide using isocyanate-terminated flexible polymer chains on the mechanical properties of epoxy composites. Journal of Materials Chemistry A. 2014;2(27):10557-67.
[15] Li Z, Wang RG, Young RJ, Deng LB, Yang F, Hao LF, et al. Control of the functionality of graphene oxide for its in epoxy nanocomposites application. Polymer. 2013;54(23):6437-46.
[16] Jiang T, Kuila T, Kim N, Ku B-C, Lee J. Enhanced mechanical properties of silanized silica nanoparticle attached graphene oxide/epoxy composites. Composites Science and Technology. 2013;79:115-25.
[17] Haeri SZ, Asghari M, Ramezanzadeh B. Enhancement of the mechanical properties of an epoxy composite through inclusion of graphene oxide nanosheets functionalized with silica nanoparticles through one and two steps sol-gel routes. Progress in Organic Coatings. 2017;111:1-12.
[18] Fang M, Zhang Z, Li JF, Zhang HD, Lu HB, Yang YL. Constructing hierarchically structured interphases for strong and tough epoxy nanocomposites by amine-rich graphene surfaces. Journal of Materials Chemistry. 2010;20(43):9635-43.
[19] Liu F, Guo K. Reinforcing epoxy resin through covalent integration of functionalized graphene nanosheets. Polymers for Advanced Technologies. 2014;25(4):418-23.
[20] Guan L-Z, Wan Y-J, Gong L-X, Yan D, Tang L-C, Wu L-B, et al. Toward effective and tunable interphases in graphene oxide/epoxy composites by grafting different chain lengths of polyetheramine onto graphene oxide. Journal of Materials Chemistry A. 2014;2(36):15058-69.
[21] Ferreira FV, Brito FS, Franceschi W, Simonetti EAN, Cividanes LS, Chipara M, et al. Functionalized graphene oxide as reinforcement in epoxy based nanocomposites. Surfaces and Interfaces. 2018;10.
[22] Chhetri S, Adak NC, Samanta P, Murmu NC, Hui D, Kuila T, et al. Investigation of the mechanical and thermal properties of l-glutathione modified graphene/epoxy composites. Composites Part B: Engineering. 2018;143:105-12.
[23] Liu F, Wu L, Song Y, Xia W, Guo K. Effect of molecular chain length on the properties of amine-functionalized graphene oxide nanosheets/epoxy resins nanocomposites. RSC Advances. 2015;5(57):45987-95.
[24] Zhang D-D, Zhao D-L, Yao R-R, Xie W-G. Enhanced mechanical properties of ammonia-modified graphene nanosheets/epoxy nanocomposites. RSC Advances. 2015;5(36):28098-104.

[25] Yu JW, Jung J, Choi Y-M, Choi JH, Yu J, Lee JK, et al. Enhancement of the crosslink density, glass transition temperature, and strength of epoxy resin by using functionalized graphene oxide co-curing agents. Polymer Chemistry. 2016;7(1):36-43.
[26] Wang X, Xing W, Zhang P, Song L, Yang H, Hu Y. Covalent functionalization of graphene with organosilane and its use as a reinforcement in epoxy composites. Composites Science and Technology. 2012;72(6):737-43.
[27] Yu G, Wu P. Effect of chemically modified graphene oxide on the phase separation behaviour and properties of an epoxy/polyetherimide binary system. Polymer Chemistry. 2014;5(1):96-104.
[28] Zhou Y, Li L, Chen Y, Zou H, Liang M. Enhanced mechanical properties of epoxy nanocomposites based on graphite oxide with amine-rich surface. RSC Advances. 2015;5(119):98472-81.
[29] Liu T, Zhao Z, Tjiu WW, Lv J, Wei C. Preparation and characterization of epoxy nanocomposites containing surface□modified graphene oxide. Journal of Applied Polymer Science. 2014;131(9).
[30] Kim K-S, Jeon I-Y, Ahn S-N, Kwon Y-D, Baek J-B. Edge-functionalized graphene-like platelets as a co-curing agent and a nanoscale additive to epoxy resin. Journal of Materials Chemistry. 2011;21(20):7337-42.
[31] Lerf A, He H, Forster M, Klinowski J. Structure of Graphite Oxide Revisited Ⅱ. The Journal of Physical Chemistry B. 1998;102(23):4477-82.
[32] Hermanson GT. Chapter 2 - Functional Targets for Bioconjugation. Bioconjugate Techniques (Third edition). Boston: Academic Press; 2013. p. 127-228.
[33] Hummers WS, Offeman RE. Preparation of Graphitic Oxide. Journal of the American Chemical Society. 1958;80(6):1339-.
[34] Tang L-C, Wan Y-J, Yan D, Pei Y-B, Zhao L, Li Y-B, et al. The effect of graphene dispersion on the mechanical properties of graphene/epoxy composites. Carbon. 2013;60:16-27.
[35] Wan Y-J, Gong L-X, Tang L-C, Wu L-B, Jiang J-X. Mechanical properties of epoxy composites filled with silane-functionalized graphene oxide. Composites Part A: Applied Science and Manufacturing. 2014;64:79-89.
[36] Jia Z, Feng X, Zou Y. Graphene Reinforced Epoxy Adhesive For Fracture Resistance. Composites Part B: Engineering. 2018;155:457-62.

[37] Zhang Y, Wang Y, Yu J, Chen L, Zhu J, Hu Z. Tuning the interface of graphene platelets/epoxy composites by the covalent grafting of polybenzimidazole. Polymer. 2014;55(19):4990-5000.
[38] Galpaya D, Wang M, George G, Motta N, Waclawik E, Yan C. Preparation of graphene oxide/epoxy nanocomposites with significantly improved mechanical properties. Journal of Applied Physics. 2014;116(5):053518.
[39] Hussein A, Sarkar S, Oh D, Lee K, Kim B. Epoxy/p□phenylenediamine functionalized graphene oxide composites and evaluation of their fracture toughness and tensile properties. Journal of Applied Polymer Science. 2016;133(34).
[40] Chandrasekaran S, Sato N, Tölle F, Mülhaupt R, Fiedler B, Schulte K. Fracture toughness and failure mechanism of graphene based epoxy composites. Composites Science and Technology. 2014;97:90-9.
[41] Wang F, Drzal LT, Qin Y, Huang Z. Enhancement of fracture toughness, mechanical and thermal properties of rubber/epoxy composites by incorporation of graphene nanoplatelets. Composites Part A: Applied Science and Manufacturing. 2016;87:10-22.

List of Tables

Table 1: Thermal properties of Epoxy, Epoxy/GO and Epoxy/GO-g-PAA nanocomposites

Sample	T_g[a] (°C)	$T_{-5\%}$[b] (°C)	Storage modulus at 150 °C (MPa)	Storage modulus at 200 °C (MPa)	Storage modulus at 250 °C (MPa)
Epoxy	280.7	302	3197	3013	1794
Epoxy/GO (0.35 wt%)	281.3	333	3296	2343	2233
Epoxy/GO (0.7 wt%)	280.9	341	3127	2890	2078
Epoxy/GO (1.05 wt%)	277.6	330	3145	2991	1983
Epoxy/GO (1.4 wt%)	277.1	309	2787	2830	1796
Epoxy/GO-g-PAA (0.35 wt%)	282.7	323	3641	3445	2473
Epoxy/GO-g-PAA (0.7 wt%)	282.5	326	4285	4108	2791
Epoxy/GO-g-PAA (1.05 wt%)	282.8	324	3715	3521	2494
Epoxy/GO-g-PAA (1.4 wt%)	283.8	303	3367	3185	2371

[a]T_g -Glass transition temperature.
[b]$T_{-5\%}$-Temperature for 5% weight loss.

List of Figures

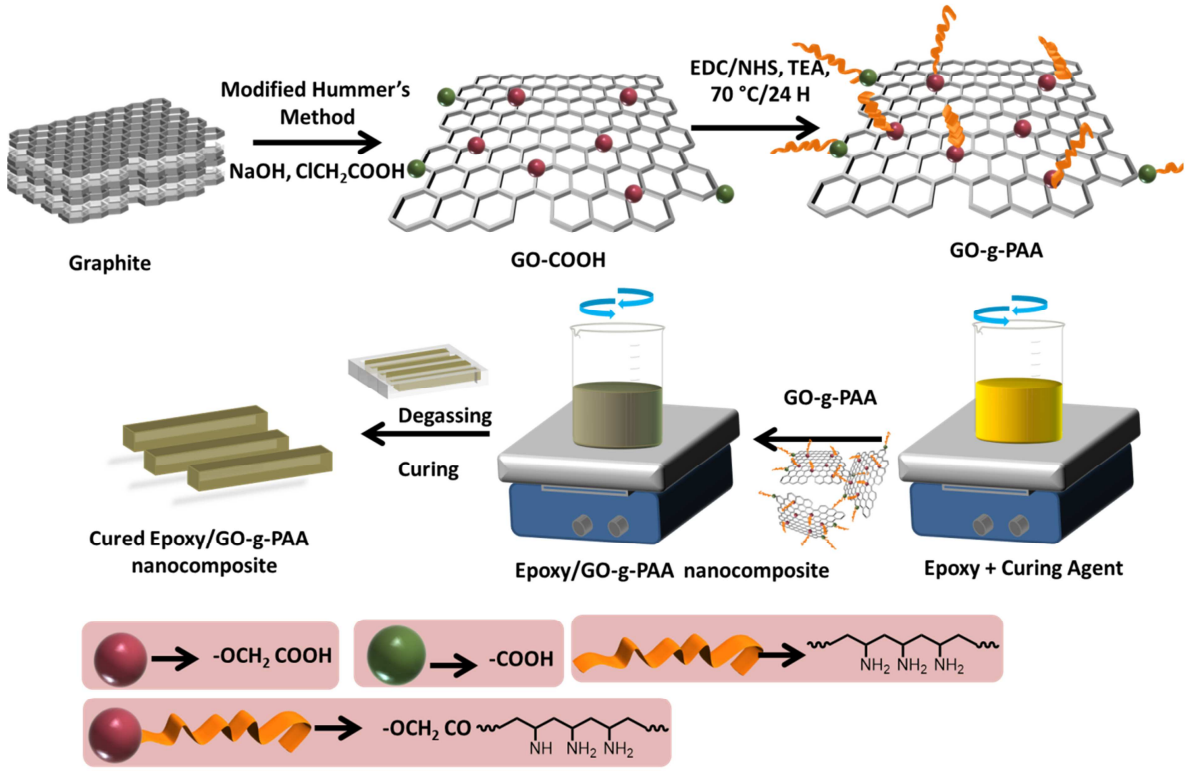

Figure 1: Schematic illustration of synthesis route fo GO-g-PAA and fabrication of GO-g-PAA modified epoxy nanocomposites.

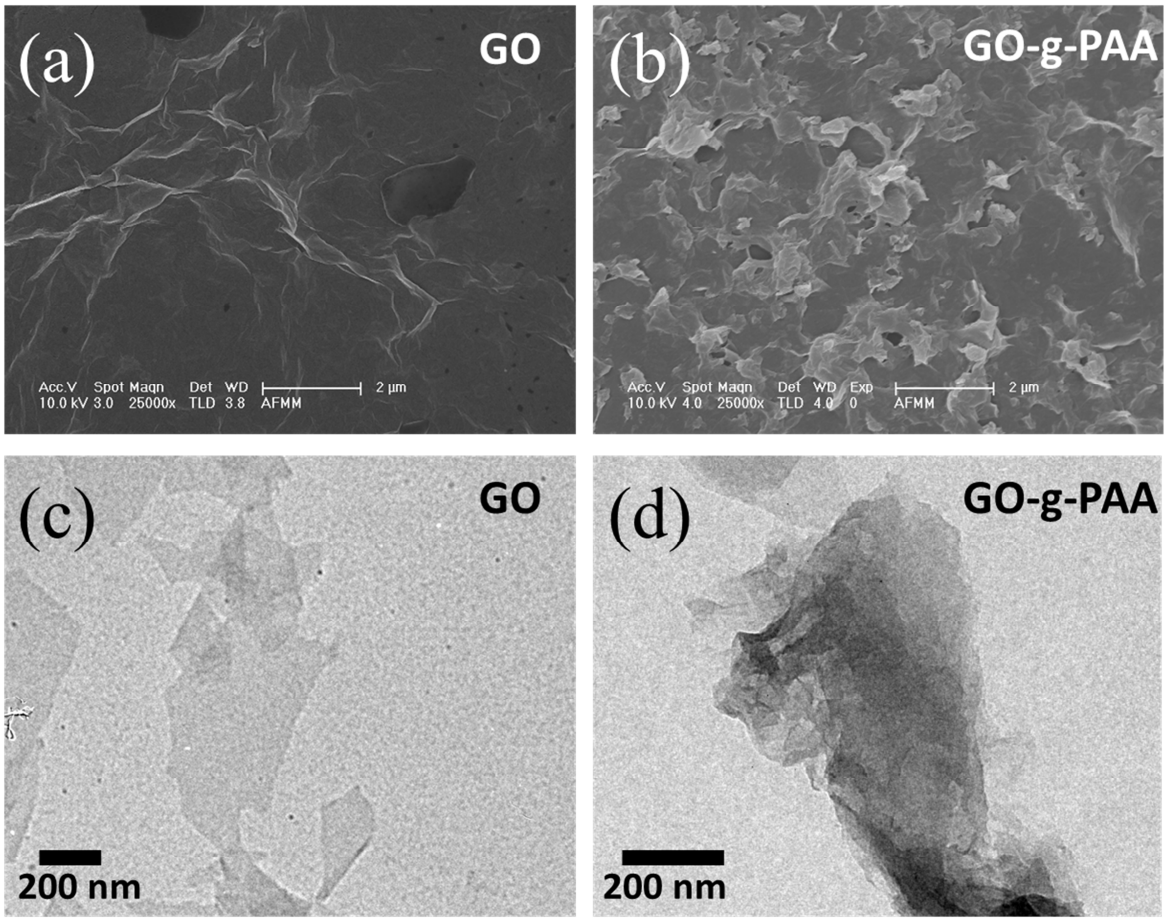

Figure 2: SEM micrographs of (a) GO and (b) GO-g-PAA. TEM micrographs of (c) GO and (d) GO-g-PAA.

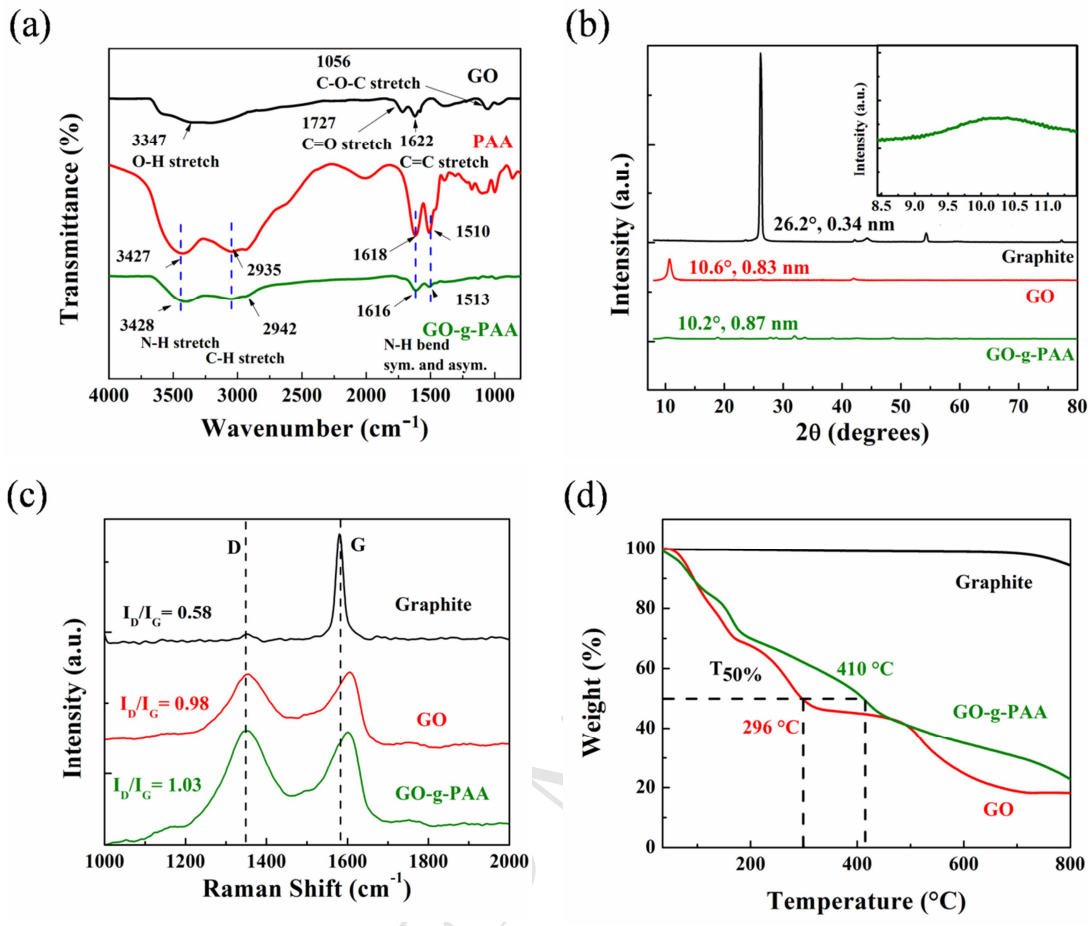

Figure 3: (a) FTIR spectra, (b) XRD patterns, (c) Raman spectra and (d) TGA plots of GO and GO-g-PAA.

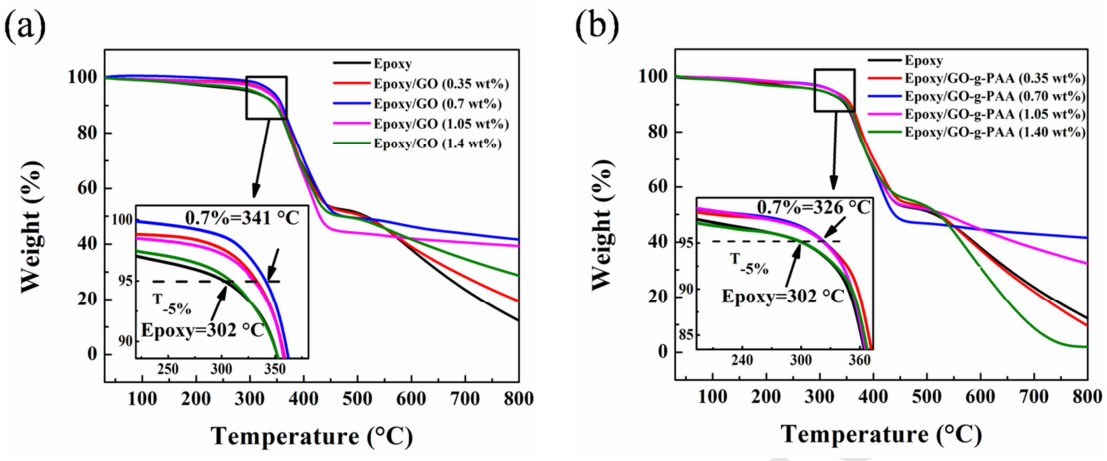

Figure 4: Comparison of TGA plot of neat epoxy with TGA plots of (a) GO and (b) GO-g-PAA modified epoxy nanocomposites.

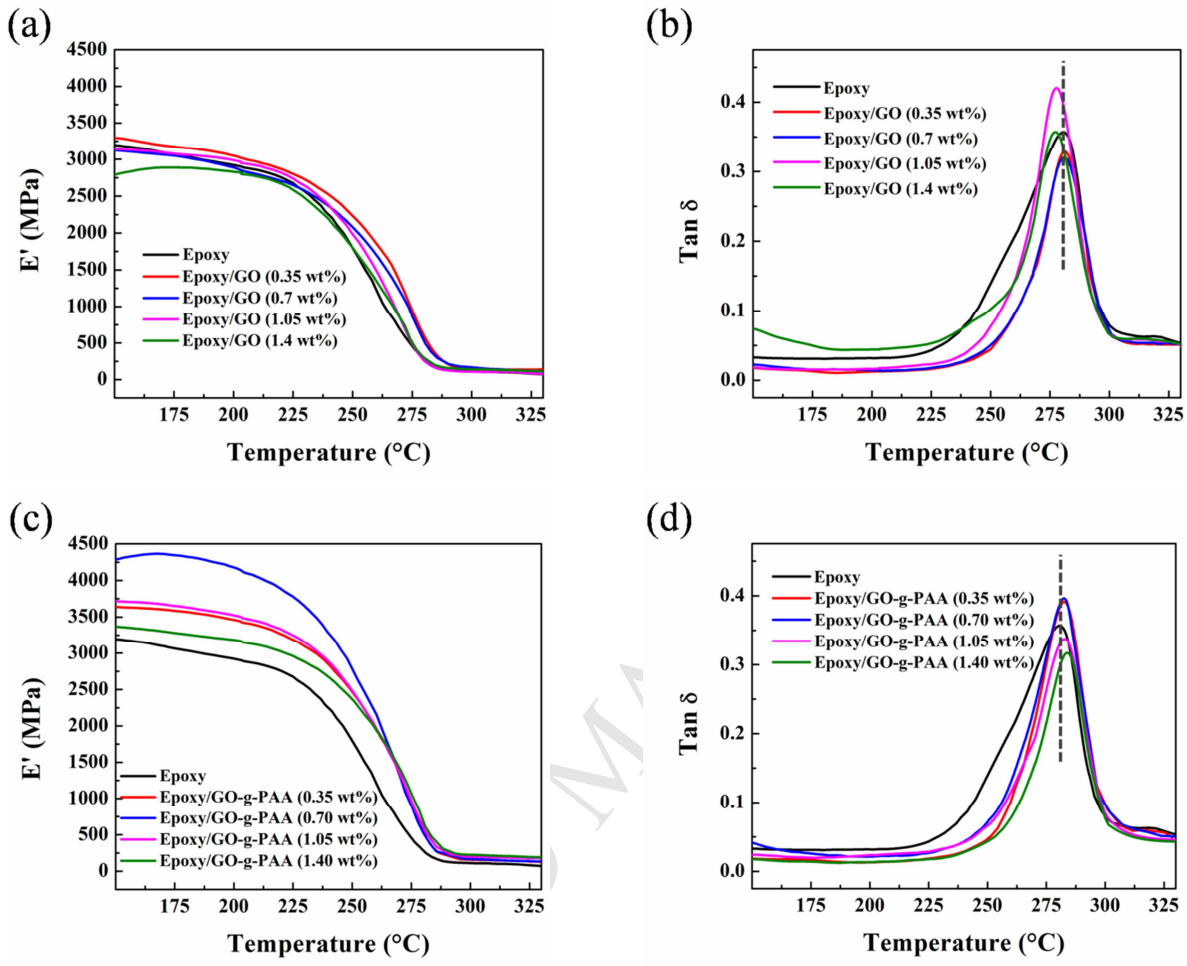

Figure 5: (a) Storage modulus and (b) tan δ as a function of temperature of Epoxy and Epoxy/GO nanocomposites. (c) Storage modulus and (d) tan δ as a function of temperature of Epoxy and Epoxy/GO-g-PAA nanocomposites.

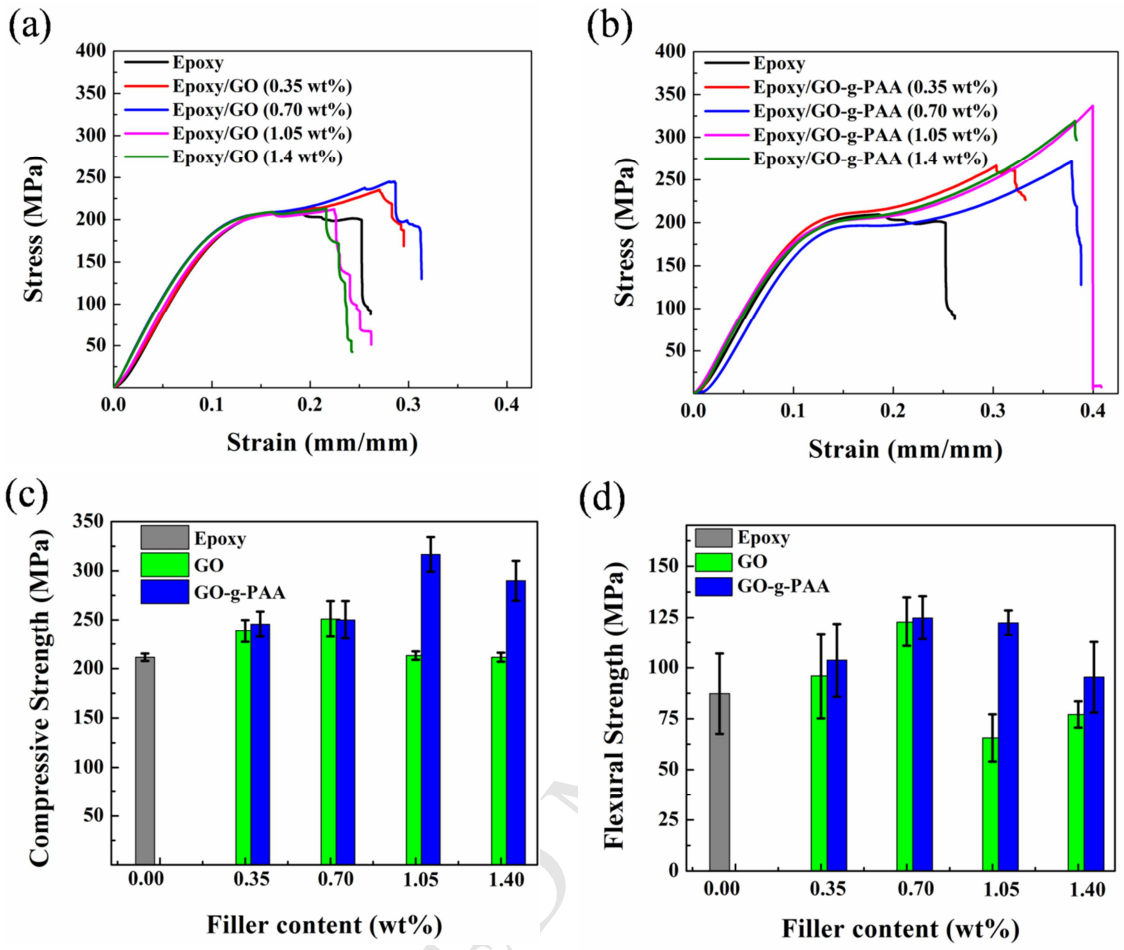

Figure 6: Typical stress versus strain curves from compression test of (a) GO and (b) GO-g-PAA modified epoxy nanocomposites. (c) Compressive strength and (d) flexural strength as a function of GO and GO-g-PAA content of epoxy nanocomposites.

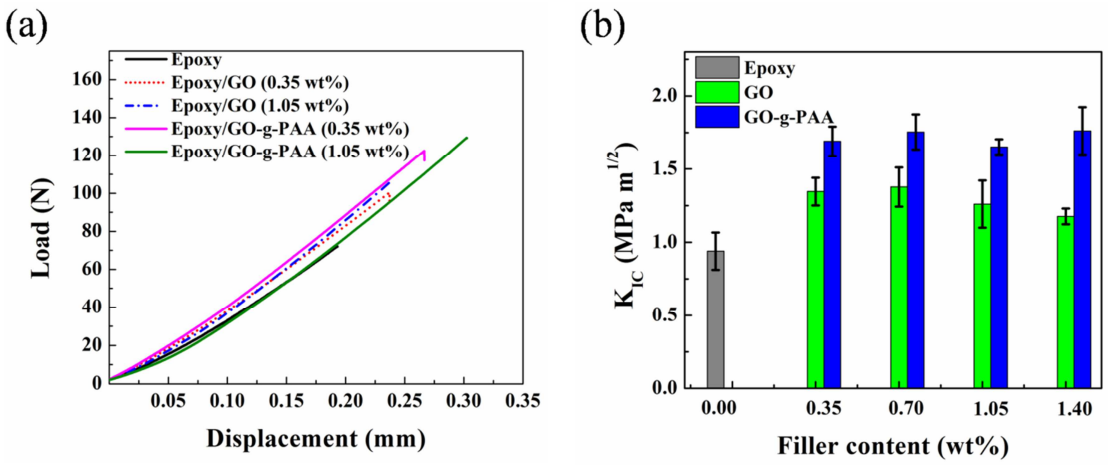

Figure 7: (a) Typical load vs. displacement curves of fracture toughness test and (b) K_{IC} as a function of GO and GO-g-PAA content of epoxy nanocomposites.

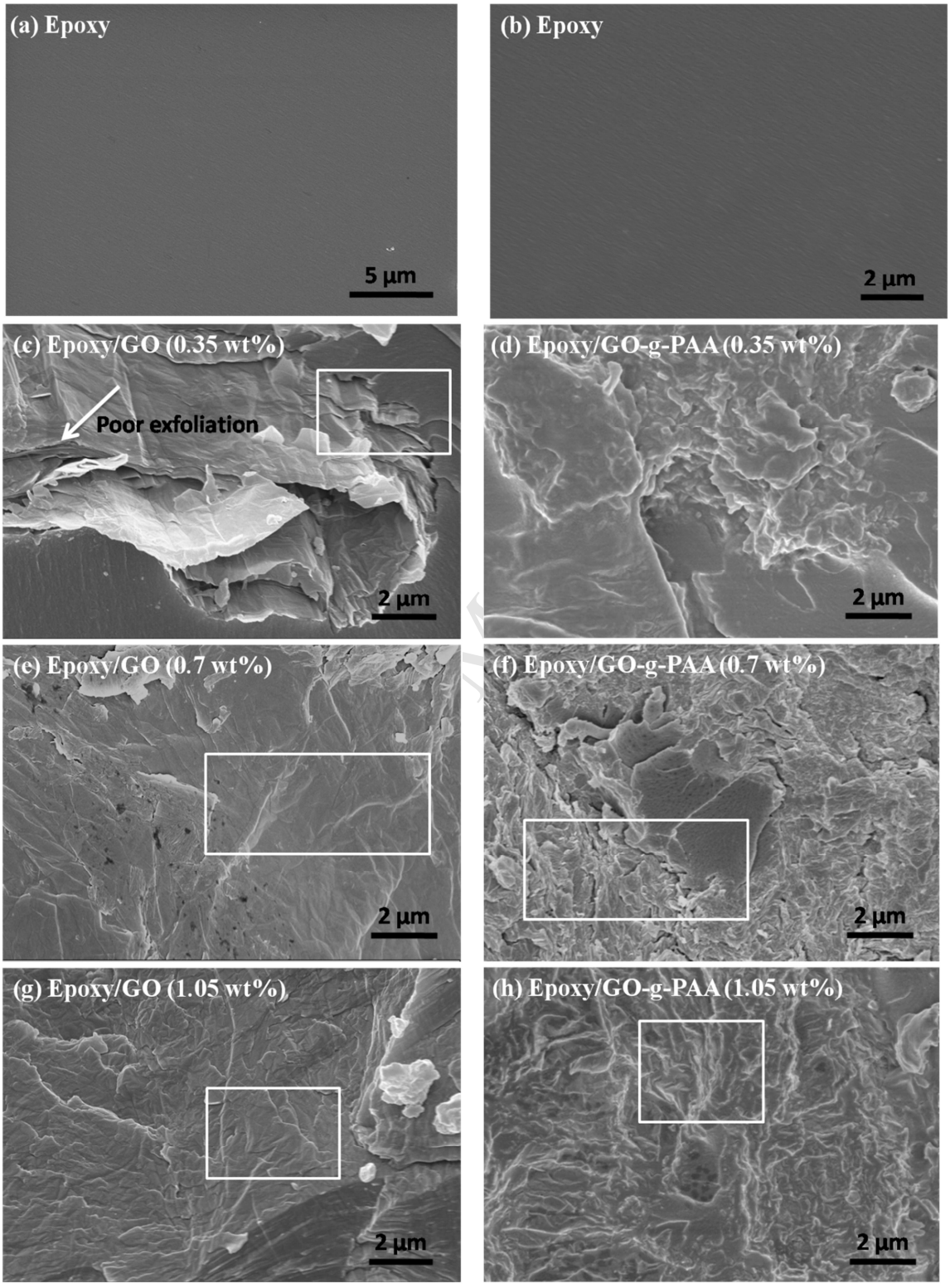
(a) Epoxy
5 µm
(b) Epoxy
2 µm
(c) Epoxy/GO (0.35 wt%)
Poor exfoliation
2 µm
(d) Epoxy/GO-g-PAA (0.35 wt%)
2 µm
(e) Epoxy/GO (0.7 wt%)
2 µm
(f) Epoxy/GO-g-PAA (0.7 wt%)
2 µm
(g) Epoxy/GO (1.05 wt%)
2 µm
(h) Epoxy/GO-g-PAA (1.05 wt%)
2 µm

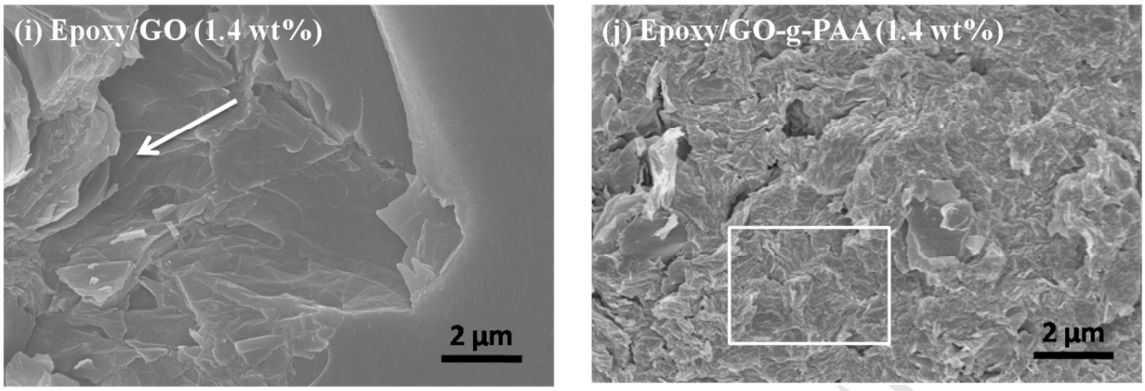

Figure 8: SEM fractographs of the neat epoxy (a, b) and nanocomposites (c, d) 0.35 wt%, (e, f) 0.7 wt%, (g, h) 1.05 wt% and (i, j) 1.4 wt% of Epoxy/GO and Epoxy/GO-g-PAA.

Table of Contents Graphic